ISSN 1392 - 1207. MECHANIKA. 2013 Volume 19(4): 478-485

Thermal structure design and analysis of a machine tool headstock

J.F. Zhang*, P.F. Feng, Z.J. Wu***, D.W. Yu****, C. Chen*******
**Tsinghua University, State Key Lab of Tribology, Beijing 100084, P.R. China, E-mail: zhjf@tsinghua.edu.cn*
***Tsinghua University, State Key Lab of Tribology, Beijing 100084, P.R. China, E-mail: fengpf@tsinghua.edu.cn*
****Tsinghua University, State Key Lab of Tribology, Beijing 100084, P.R. China, E-mail: wuzhijun@tsinghua.edu.cn*
*****Tsinghua University, State Key Lab of Tribology, Beijing 100084, P.R. China, E-mail: yudw@tsinghua.edu.cn*
******Tsinghua University, State Key Lab of Tribology, Beijing 100084, P.R. China, E-mail: ccyxql@gmail.com*

crossref http://dx.doi.org/10.5755/j01.mech.19.4.5044

1. Introduction

The influence of errors imposed on workpiece by thermal deformation of machine tools has attracted wide attention. Studies have shown that 40–70% of the error in precision machining arises from thermal error [1-3]. It has become one of the most important research topics to fully consider the thermal performance optimized design in the machine tool design stage and to improve the machining precision. In recent years, the optimization methods for machine tool thermal performance can be divided into three categories.

One is structural optimization design for thermal characteristics. It optimizes or redesigns the structure of the key parts without changing the heating power of the thermal source of the machine tool, which results in a more uniform temperature distribution inside the machine tool. The thermal deformation generated between the spindle and the workbench caused by thermal expansion can mutually cancel each other, resulting in reduced thermal error and improved machining precision. The basic design theory is the "thermal plane of symmetry". And the finite-element method is one of the main approaches for complex-structure machine tool thermal performance analysis and structural optimization research [4].

Another is temperature control. By controlling the magnitude and distribution of the temperature for key parts, the objective of reducing spindle thermal deformation relative to the workbench can be achieved. Two major temperature control methods are installing heating components or installing cooling systems on the machine tool. The ultimate goal of both approaches is to achieve a balanced temperature field, reducing the thermal deformation of the machine tool [5]. At present, a widely adopted and effective method is forced cooling using cooling oil to remove the spindle-generated heat such that the thermal deformation of the machine tool is reduced.

The third is thermal deformation modeling and compensation. It is a method to improve machining precision during the cutting process after the machine tool design and manufacture are finished. The implementation of this method includes using experimental measurements on machine tool thermal deformation and temperature fields at the early stage, building the thermal deformation model using mathematical methods, and performing real-time compensation using NC programs. The major modeling methods include multivariable linear regression [6], many-body theory [7], the artificial neural network method [8], and gray system theory [9]. The real-time compensation methods are commonly used for performance improvement of machine tools [10-13].

This paper mainly adopted proactive control methods to optimize the thermal performance and reconstruct the headstock of a vertical machining center. Therefore, a combination of methods using structural optimization design of thermal characteristics and temperature control are used to perform virtual evaluations of thermal performance for designed models, satisfy the required thermal performance constraints, and achieve a satisfactory effect. And by adopting the finite-element method to optimize the design parameters during the prototype design stage, it can also reduce a large amount of the experimental verification effort and development cost. One aspect is that of thermal performance structural optimization design, aimed at the weakest factor affecting the thermal performance (the headstock), which resulted in the conversion of the originally asymmetric structure to a symmetric structure in the X-direction. The other approach is to build thermal-conduct troughs on both sides and the front of the headstock. By injecting cooling fluid into the troughs, we can cool the headstock and spindle, consequently reducing the temperature and thermal deformation of the entire vertical machining center.

2. Thermal performance weakness analysis and reconstruction scheme of a machine tool headstock

2.1. Thermal performance weakness analysis

The identification and control of the thermal weaknesses were done through finite-element thermal performance simulation analysis. For the finite-element simulation of the temperature field and the thermal deformation of the vertical machining center, the thermal sources, the heat transfer boundary conditions including heat transfer coefficient and thermal contact resistance, and the thermophysical parameters of various machine tool materials were firstly determined. Based on the constructed simulation models, the whole-machine finite-element simulated temperature field distribution and thermal deformation are shown in Fig. 1. As shown in the figure, heat was mainly concentrated around the spindle component and headstock, and a small portion of the heat was transferred to the column through the slider and rails due to the existence of joint thermal conduct resistance, although the column temperature elevation was very small. In addition, the temperature elevation was more significant at positions on the headstock and close to the spindle bearing and motor.

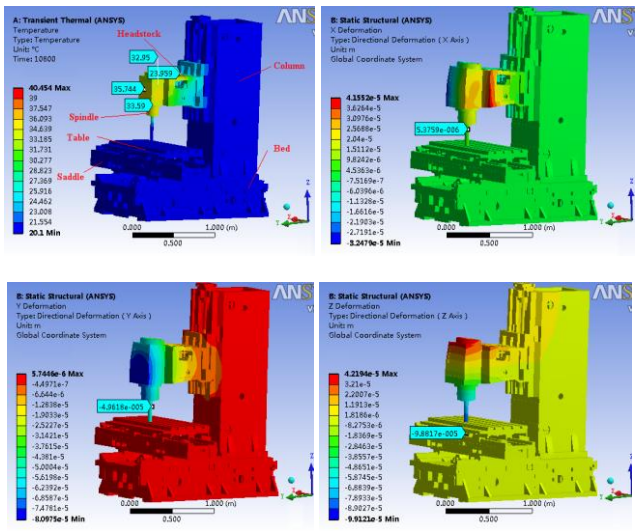

Fig. 1 Temperature field distribution and thermal deformation in X-, Y- and Z-direction

The machine tool used a mechanical spindle for which the maximum rotational speed was 8000 rpm, and the spindle itself did not have a cooling circulation system. The spindle bearing radiated intense heat. This heat was transferred from the spindle to the surface of the headstock, where it relied on the natural convection of air for cooling. However, the cooling effect was insufficient, and the spindle components accumulated a large amount of heat and became significantly deformed. Due to the spindle sleeve, headstock hole, and headstock anterior wall are thin-walled structures, their temperature gradients became very large because of the internal heating of the spindle. On the one hand, these structures were inclined to expand because of the heat; on the other hand, they helped to create thermal flexion and extension because of the inconsistent thermal deformation caused by temperature differences as a result of thermal contact resistance. Comparing the thermal deformation along various axes, the sequence of directions along which deformation increased was the X-direction (5.3 μm), the Y-direction (49.6 μm), and the Z-direction (98.8 μm). The main forms of thermal deformation affecting the machining precision were thermal expansion deformation and up-and-down movement along the Y-Z plane. Therefore, it can be concluded that the thermal performances in the Y-direction and Z-direction were the weakest links.

Because the headstock was asymmetry in the X-direction, it was the major cause of the spindle shaft end thermal deformation in the X-direction. However, the headstock size in X-axis dimension is relatively small, and therefore, the thermal expansions in the X-positive and X-negative directions can partly offset each other. The thermal deformation generated was much smaller compared with the thermal deformation in the Y- and Z-directions. Because the headstock size in the Y-direction was large and consisted of a cantilever structure, the thermal expansion in this direction was significantly greater than the expansion in the X-direction. The spindle motor was installed in the top middle position of the headstock. No other cooling devices were installed to facilitate the dissipation of heat, and therefore, the dissipation occurred only through the natural convective heat transfer to the air. The thermal deformation of the machine tool, coupled with each of the heated parts, caused an extreme temperature elevation for the anterior and central parts of the headstock and enhanced the thermal deformation in the Y-direction.

The main type of deformation exhibited in the Z-direction was expansion in the negative direction along the Z-axis. This result occurred because the spindle had a very large Z-direction dimension size. The heated spindle caused an elevated temperature in the spindle components. Therefore, the thermal expansion of the spindle components in the Z-direction caused the machine tool to experience greater thermal deformation in the Z-direction. In addition, the heat generated by the spindle bearing was transferred to the headstock, where it overlapped with the heat generated by the spindle motor. The thermal expansion and contraction generated in the headstock in the Z-direction also increased the heat deformation in the Z-direction.

To summarize, the heat dissipation for the headstock structure and spindle components is a critical issue affecting the thermal performance of this vertical machining center. To limit the thermal deformation of the vertical machining center in various directions, on the one hand, we install cooling devices to control the spindle temperature rise. On the other hand, we improve the headstock structure by increasing its thermal stiffness, consequently improving the thermal performance of the vertical machining center.

2.2. Thermal structure design and reconstruction scheme of the headstock

Based on the weakness analyses of the machine tool thermal performance and for the purposes of minimizing the cost, we proposed the following thermal structure design and reconstruction scheme: 1) Install a cooling fan on top of the spindle motor to reduce the heat transfer from the motor to the headstock and at the same time perform forced cooling on the spindle motor and headstock. 2) Apply "thermal plane of symmetry" theory to the headstock, converting the asymmetric structure to a symmetric structure along the X-axis. With a symmetric temperature field inside the headstock, the whole-machine thermal deformation can be reduced. 3) Design reasonable trough structures on both sides and at the front of the headstock, injecting cooling fluid to cool the headstock and thereby lowering the temperature rise and thermal deformation of the whole-machine. 4) Counteract the loss of stiffness caused by the cooling trough optimization and satisfy the whole-machine static and dynamic optimization requirements. To accomplish this objective, add oblique ribs on the top and right sides of the bottom of the headstock to improve the inner rib structure, increase the lateral rib span, increase the fillet radius of the inner ribs, and increase the thickness of the underside of the support plate.

Three-dimensional models of the headstock before and after the reconstruction are shown in Fig. 2. Before reconstruction, the mass of the headstock was 295.2 kg; and the sizes in the X-, Y- and Z-directions were 385, 690, and 354 mm, respectively. The headstock was asymmetric along the X-axis. There were two oblique ribs on both the left and lower sides. There was no gap between the headstock hole and the headstock anterior wall. The generated heat was transferred directly to the spindle anterior wall through the headstock hole. The average temperature elevation was greater on the anterior wall.

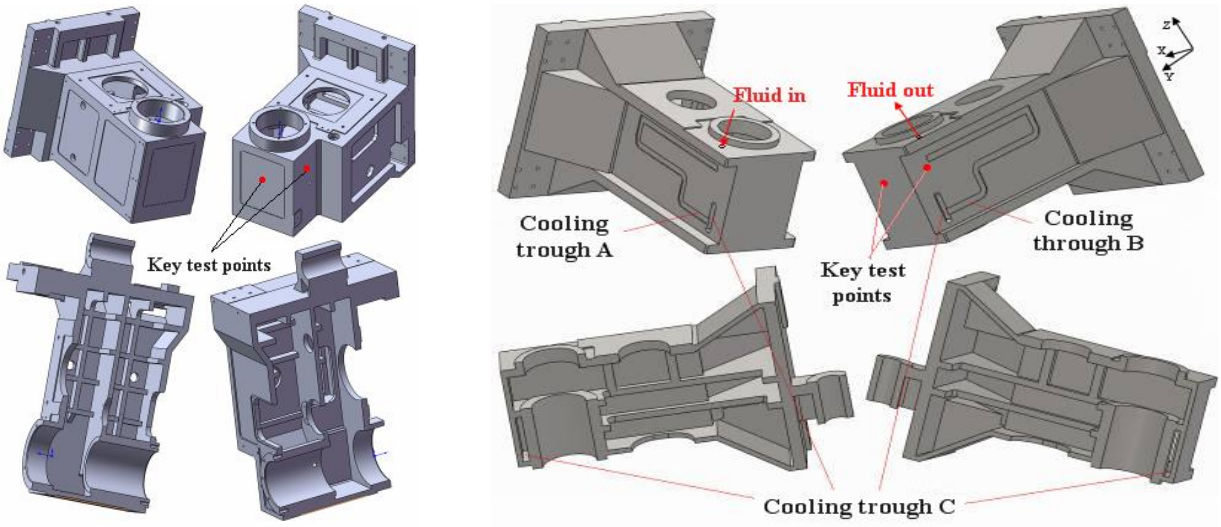

a b

Fig. 2 Three-dimensional models of the headstock before and after reconstruction: a) The original model; b) The model after reconstruction

After reconstruction, the mass was 295.3 kg; and the sizes in the X-, Y- and Z-direction were 300, 775, and 335 mm, respectively. The headstock was symmetric along the X-axis. There were four oblique ribs distributed in four directions (up, down, left, and right) at the bottom of the headstock to improve the static, dynamic, and thermal stiffness of the headstock. This structural improvement kept the headstock mass unchanged, reduced the size in the X- and Z-directions, and increased the size in the Y-direction. According to stiffness analyses, it showed that the static and dynamic performances of the headstock were improved significantly. Based on thermal expansion theory, when the spindle bearing was heated, the heat received in the lower part was greater than the heat received in the upper part. On the one hand, the headstock experienced thermal expansion and deformation in the Z-direction; on the other hand, because one end of the headstock was fixed, the heat generated at this end was dissipated. The larger the size in the Y-direction, the bigger the values would be because of the upturning of the front end of the headstock in the Z-direction. Due to the changes in size of the headstock in the Y- and Z-directions, the thermal deformation of the machine tool in the Z-direction would decrease, and the deformation in the Y-direction would increase.

The rectangular cooling troughs A and B (20 mm wide and 4 mm thick) were designed symmetrically on both sides of the headstock. Cooling trough C was designed between the headstock hole and the headstock anterior wall. The height of cooling trough C was 148 mm. Its minimum width of 18 mm was the shortest distance between the exterior wall of the headstock hole and the inner wall of the headstock anterior wall. Because the thermal contact resistance for thermal transfer from the headstock hole to the headstock anterior wall was increased, the average temperature elevation of the headstock anterior wall was decreased, and the thermal deformation was reduced. When the circulating cooling system was in operation, the cooling fluid flowed into the cooling trough A on the left side from the position of the spindle to the position of the motor along the negative Y-direction, and the length of this section was 380 mm. Then, from the position of the motor to the position in the middle of the headstock in the negative Z-direction, the length of the section was 80 mm. The cooling fluid then flowed near the spindle in the positive Y-direction, and the length of this section was 240 mm. The fluid then flowed to the bottom of the headstock, and the length of this section was 90 mm. It then flowed to the entrance of cooling trough C in the positive Y-direction, and the length of this section was 150 mm. The cooling fluid flowed through cooling trough C and into the entrance of cooling trough B. Its flow path inside cooling trough B was symmetric with cooling trough A. When the cooling fluid was flowing in cooling troughs A, B, and C, it transmitted the heat away from the headstock. Consequently, the temperature of the headstock and thermal deformation of the vertical machining center can be reduced by this kind of structure design.

3. Thermal performance analysis of the machine tool after headstock reconstruction

3.1. Heat transfer analysis of the cooling trough for the reconstructed headstock model

When the fluid flowed inside the rectangular cooling trough of the headstock, forced convection heat transfer occurred between the cooling fluid and the headstock. Based on forced convection heat transfer theory, the flow states of the cooling fluid inside the rectangular trough were categorized as laminar flow state, transition state, and turbulent state. These different flow states corresponded to different coefficients in the empirical formula describing the heat transfer. The flow states for the fluid in the trough can be judged based on the fluid Reynold's number [14], Re, as shown in Eq. (1):

$$Re = \frac{u D_H}{\nu}, \tag{1}$$

where D_H is the equivalent diameter of the rectangular trough in units of m, u is the characteristic velocity of the cooling fluid in units of m/s, and ν is the kinematic viscosity of the fluid in units of m^2/s.

When $Re < 2000$, the cooling fluid inside the trough is in a strict laminar flow state, mostly caused by the small inner radius, the low temperature difference, and the high viscosity of the cooling fluid. At this time, if $Re \cdot Pr \cdot D_H / L > 10$ and $Pr > 0.6$, then the Nusselt number of the fluid can be calculated using Eq. (2) [15]:

$$Nu = 1.86\left(Re \cdot Pr \frac{D_H}{L} \right)^{1/3}, \quad (2)$$

where the Prandtl number, Pr, reflects the physical parameters of the coolant and can be calculated using Eq. (3):

$$Pr = \frac{c_p \rho v}{\lambda}. \quad (3)$$

When $2000 < Re < 4000$, then the cooling fluid in the rectangular trough is in a state of transition from laminar flow to steady flow, and its Nusselt number can be calculated using Eq. (4) [15-17]:

$$Nu = 0.116\left(Re^{2/3} - 125 \right) Pr^{1/3} \times \times \left[1 + \left(\frac{D_H}{L} \right)^{2/3} \right] \left(\mu_f / \mu_w \right)^{0.14}, \quad (4)$$

where μ_f is the dynamic viscosity of the cooling fluid at the average temperature in units of Pa·s and μ_w is the dynamic viscosity of the cooling fluid at the wall temperature in units of Pa·s.

When $Re > 4000$, the cooling fluid in the trough is in a state of turbulence, and if, at the same time, $0.7 < Pr < 120$ and $L / D_H \geq 60$, then the Nusselt number of the fluid can be calculated using Eq. (5):

$$Nu = 0.023 Re^{0.8} Pr^{0.4}. \quad (5)$$

The forced convection heat transfer coefficient of the cooling fluid inside the rectangular trough α can be calculated using Eq. (6):

$$\alpha = \frac{Nu \lambda}{D_H}. \quad (6)$$

The equivalent diameters for the above formula can be calculated using Eq. (7):

$$D_H = \frac{4A}{U}, \quad (7)$$

where A is the cross-sectional area of the cooling trough in units of m^2 and U is the wetted perimeter in units of m.

The cooling system of the vertical machining center is an oil cooler machine entitled Taiwan HBO–750PSA. The oil cooler power P was 2500 W, and the pump flow volume was 25 L/min. PT300 long-life emulsion was adopted as the cooling fluid for the cooling trough circulation cooling system; the kinematic viscosity of this fluid v was 32 mm^2/s at 40°C, the density ρ was 876 kg/m^3, the thermal conductivity λ was 0.144 W/(m·K), and the specific heat capacity c_p was 1955 J/(kg·K). Based on the above data and formulas, we derived various parameters necessary for calculating the convective heat transfer coefficient between the cooling trough and the cooling fluid (as shown in Table 1).

Table 1
Calculation of the convective heat transfer coefficient

	Values	Equation	Description
A	0.8×10^{-4} m^2		Channel cross-sectional area
U	4.8×10^{-2} m		Wetting perimeter
D_H	0.667×10^{-2} m	(7)	Equivalent diameter
u	5.21 m/s		Characteristic velocity
v	32×10^{-6} m^2/s		Kinematic viscosity
Re	1086	(1)	Reynolds number
c_p	1955 J/(kg·K)		Specific heat capacity
ρ	876 kg/m^3		Density
λ	0.144 W/(m·K)		Thermal conductivity
Pr	380.6	(3)	Prandtl number
L	0.94 m		Rectangular trough length
Nu	26.6	(4)	Nusselt number
α	574.3 $W/(m^2 \cdot K)$	(6)	Convective heat transfer coefficient

3.2. Thermal performance simulations of the machine tool considering fluid/structure interaction

By replacing the headstock model in the whole-machine assembly and considering the cooling effect of the cooling trough, we performed a simulation analysis of the whole-machine thermal performance of the vertical machining center after structural reconstruction. Take the spindle rotational speed of 6000 rpm as an example, the whole-machine thermal performance modeling and simulation boundary conditions were calculated and set as follows: the single bearing heat power was 52.1 W; the forced-convection heat transfer coefficients of rotation surface of the spindle and tool shank and test bar surface were 158.8 and 126.0 $W/m^2 \cdot K$; composite heat transfer coefficient between stationary surfaces, such as headstock, column, table, saddle and bed, and the air/environment was 9.7 $W/m^2 \cdot °C$; thermal contact resistances of key machine tool joints surface between test bar-holder and spindle taper hole, bearing inner ring and spindle, bearing outer ring and spindle sleeve, spindle sleeve and headstock, and guideways between headstock and column were 2.00×10^{-3}, 1.37×10^{-4}, 6.06×10^{-4}, 1.13×10^{-3}, and 1.67×10^{-3} $m^2 \cdot °C/W$, respectively; convective heat transfer coefficient of the cooling trough was 574.3 $W/m^2 \cdot K$, and the material thermophysical property was 20Cr, 45# steel used for machine spindle parts, and the material used for machine components (such as the headstock, column, table, saddle, bed) was HT300. The whole-machine initial temperature and environment temperature set to 24.3°C, and the whole-machine thermal performance simulation results including temperature field distribution and three-axis thermal deformation were shown in Fig. 3.

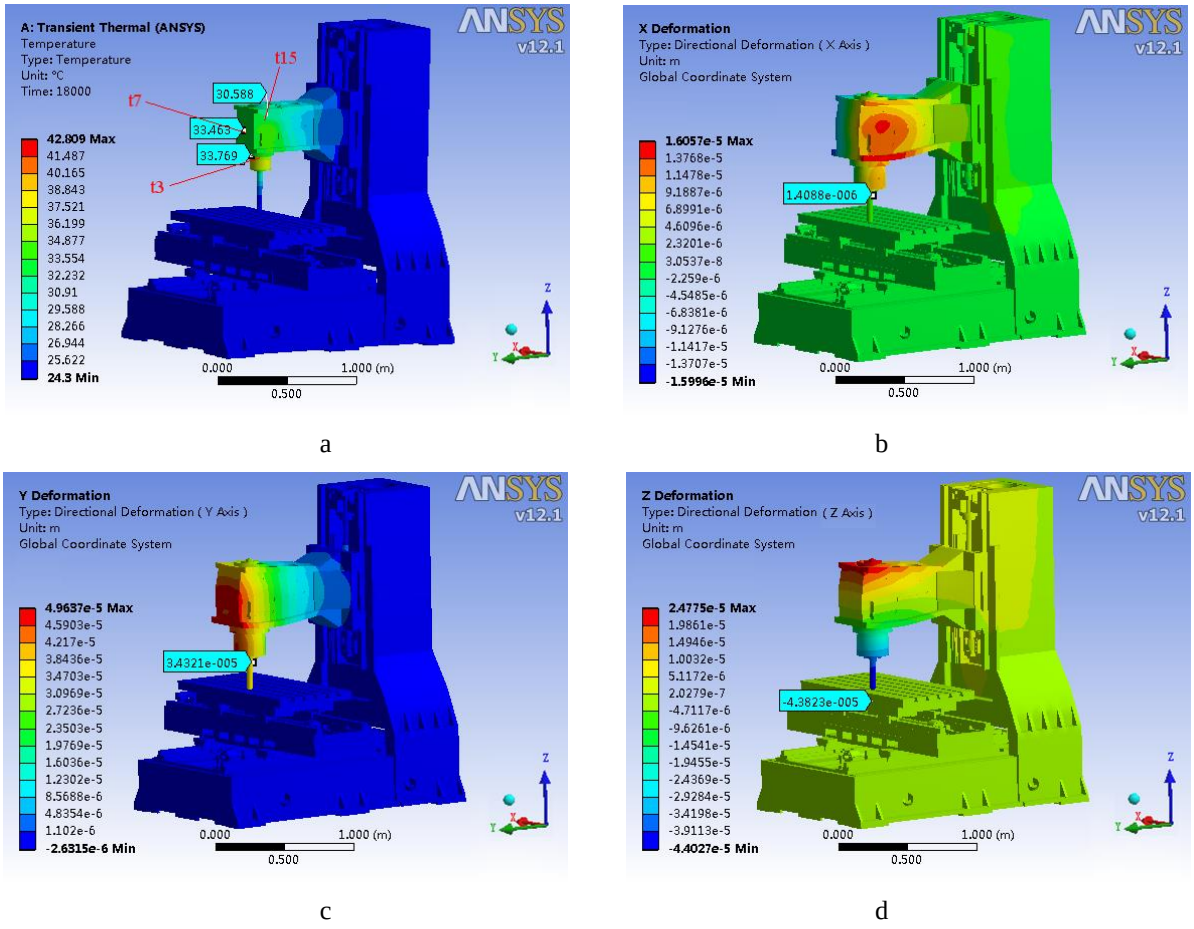

Fig. 3 Thermal performance simulation results at 6000 rpm after the reconstruction: a) Whole-machine temperature field; b) Thermal deformation in X-direction; c) Thermal deformation in Y-direction; d) Thermal deformation in Z-direction

The simulation results for the temperature elevation of the critical points and the thermal deformation before and after the reconstruction are compared in Tables 2 and 3. As is shown, after introducing the cooling function of the headstock cooling trough, the whole-machine thermal performance of the vertical machining center improved significantly. The temperature elevation at the front surface of the headstock around the spindle bearing (upper and lower points) and at points on the side of the headstock decreased by 29.7%, 41.4%, and 51.1%, respectively, compared with their values of the original structure. At the same time, the thermal deformation in the X-, Y- and Z-directions decreased 73.8%, 30.8%, and 55.7%, respectively, after the reconstruction.

Table 2

Comparison of the temperature field simulation results before and after the reconstruction

Spindle speed, rpm	No. of the critical temperature measuring points	Simulation values, °C (Before reconstruction)		Simulation values, °C (After reconstruction)		Reduction in temperature elevation
		Initial temperature	Finish temperature	Initial temperature	Finish temperature	
6000	t3	20.1	33.59	24.3	33.78	29.7%
	t7	20.1	35.74	24.3	33.46	41.4%
	t15	20.1	32.95	24.3	30.59	51.1%

Table 3

Comparison of thermal deformation simulation results before and after reconstruction

Spindle speed, rpm	Thermal deformation direction	Deformation value, μm (Before reconstruction)	Deformation value, μm (After reconstruction)	Reduction in thermal deformation
6000	X	-5.376	-1.409	-73.8%
	Y	49.618	34.321	-30.8%
	Z	-98.817	-43.823	-55.7%

4. Experimental verification of the reconstruction scheme

According to the simulation results, a new headstock was designed and manufactured. To verify the improvement in thermal performance of the vertical machining center after reconstruction, this study adopted the machine tool thermal performance experimental method proposed in [18] to conduct experimental measurements on the whole-machine thermal properties of the vertical machining center. The test platform is shown in Fig. 4. Thirty two platinum resistance temperature sensors were fixed onto the surface of the machine tool to get the temperature distribution. Two laser displacement sensors were fixed on the worktable to measure the thermal deformation of the X and Y axes. And an eddy current displacement sensor was placed below the bottom of the spindle test bar to detect the Z-axis thermal deformation. In addition, to evaluate the whole-machine thermal performance of the vertical machining center after the reconstruction, the same thermal performance test was also done on a HAAS vertical machining center, and we used its thermal characteristic parameters as the reference system for comparison.

To use the example of a 6000 rpm spindle rotational speed, the experimental results of the temperature elevation at critical points on the vertical machining center under the same running time before and after the reconstruction are compared in Table 4. From Table 4, after the reconstruction, the measured temperature elevation at the critical points on the machine tool decreased by approximately 29.8%, 34.7%, and 49.6%, respectively, compared with the values obtained without reconstruction. The temperature characteristics were under better control, and the results were consistent with the simulation data.

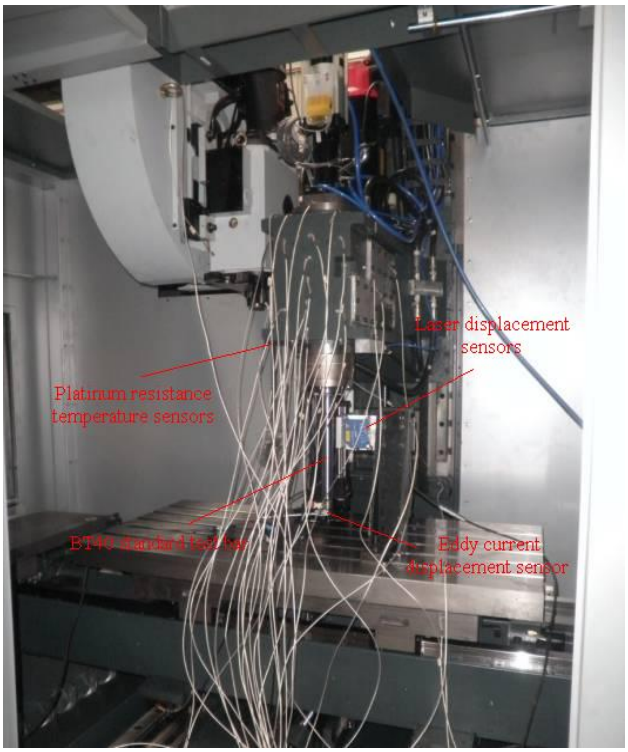

Fig. 4 The temperature field and thermal deformation test platform after the reconstruction

Table 4

Comparison of the temperature field experimental results before and after the reconstruction

Spindle speed, rpm	No. of the critical temperature measuring points	Experimental values, °C (Before reconstruction)		Experimental values, °C (After reconstruction with cooling)		Reduction in temperature elevation
		Initial temperature	Finish temperature	Initial temperature	Finish temperature	
6000	t3	20.1	33.2	24.3	33.5	29.8%
	t7	20.4	34.8	24.5	33.9	34.7%
	t15	20.6	34.3	23.3	30.2	49.6%

The displacement data acquisition system is programmed in the National Instruments LabVIEW. Because a 16-bit data acquisition card was used, the displacement measurement system could collect 1200 items of data per second in each channel. The system gets experimental data from the data acquisition card, and the data analysis and processing are carried by its specific software. The testing data processing method is that the output signal from the displacement sensors measures the geometric deformation, and then the thermal deformation data from the displacement measurement system were processed into a curve. The thermal deformation measurement curves along the X-, Y-, and Z-directions were shown in Fig. 5. They were the red curves before the reconstruction (Before Opt. -X, -Y and -Z), green curves after the reconstruction without oil cooling (After Opt. -X, -Y and -Z), black curves after the reconstruction with oil cooling (After Opt. -X, -Y and -Z (oil cooling)), and blue curves of HAAS vertical machining center (HASS -X, -Y and -Z).

Based on comparison of the thermal deformation curves at 6000 rpm shown in Fig. 5, some conclusions are drawn as follows:

1) In the X-direction, the differences in the thermal deformation values measured by four group of experimental data were minimal (the thermal deformation values in this figure were the raw data obtained through the original measurement, and the systematic errors introduced by the test device were not considered) and were no greater than 20 μm after thermal equilibrium was reached. Overall, the heating performance after the reconstruction was better than that before the reconstruction.

2) In the Y-direction, without turning on the cooling system, the optimized vertical machining center showed similar thermal deformation before and after the reconstruction within three hours of being powered on; when the cooling system was turned on, the thermal deformation was significantly reduced by approximately 30% relative to the deformation observed before the reconstruction, and this thermal performance was superior to that of the HAAS machine tool of the same type.

3) In the Z-direction, the thermal performance of the optimized vertical machining center was most evident and reached a steady state within one hour after booting. With the cooling system off, the thermal deformation steady-state value was approximately 60 μm, which was approximately 45% lower than the value obtained before the reconstruction. With the cooling system turned on, the steady-state value was approximately 43 μm, 60% lower compared with the value before the reconstruction. As with the Y-direction, the thermal performance in the Z-direction is superior to that of the HAAS machine of the same type.

From the above analyses of the experimental data, it appears that, by reconstructing the structure and adding a cooling trough to the headstock, the thermal performance of the machine tool was greatly improved, and the experimental and simulation results are in very close agreement.

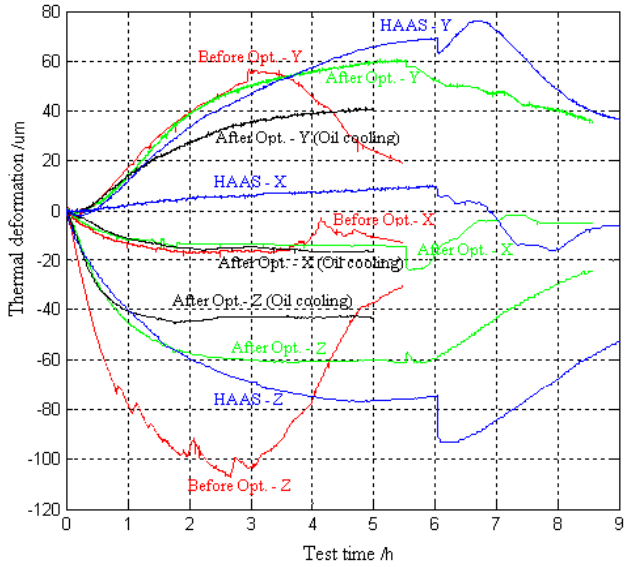

Fig. 5 Comparison of the thermal deformation curves of the whole-machine at 6000 rpm

5. Conclusion

In the digital design phase of the machine tool, by conducting the thermal structural optimization, controlling temperature levels and distribution of the key components of the machine, it can reduce the thermal deformation of the machine and improve the machining accuracy. This consideration has become one of the most critical issues in designing and manufacturing high-speed, high-precision CNC machines. In this paper, based on multiple optimization simulation runs on relevant parameters, such as the headstock structure and cooling trough layout, the selected final reconstruction scheme passed the finite-element simulation verification and the experimental prototype test verification. The thermal performance of the machine tool was improved significantly. The two main contributions of this paper are summarized below.

Firstly, based on the design requirements, through an analysis of the thermal performance weaknesses of a vertical machining center made by mass production, it presented a method to improve the machine tool thermal performance. Under the assumption that the power of the thermal source of the machine does not change, this approach resulted in the cooling of the headstock with the addition of a cooling fan near the main spindle motor, implementing a symmetric design for the headstock structure, and designing a cooling trough (adding an arch cooling trough in front of the main spindle, designing the cooling trough layout, and optimizing the width and depth dimensions of the troughs). This approach rendered the temperature more consistent inside the headstock, and reduced the temperature elevation and thermal errors of the whole-machine.

Secondly, through an analysis of the thermal transfer of the cooling trough of the headstock, the coefficient parameters were obtained for the forced convection heat exchange between the cooling troughs and the coolant, and a digital simulation model of the reconstructed machine tool was established. By comparing the thermal deformation simulation results before and after the reconstruction, the thermal performance of the reconstructed vertical machining center was shown to be improved. On this basis, the thermal performance experiments were carried out to verify the reconstruction schema. Compared with the results before the reconstruction (and with the HAAS machine tool), when turning on the circulating cooling system of the headstock, the thermal performance of the vertical machining center was found to be greatly improved, and the thermal deformations in the Y- and Z-directions were reduced by 30% and 60%, respectively.

Acknowledgements

This research was financially supported by the Key National Science and Technology Projects of China (Grant No. 2012ZX04010-011 and 2012ZX04002-061) and the State Key Laboratory of Tribology Foundation (Grant No. SKLT11C7).

References

1. **Zhou, J.L.** 2001. Research on control and prevention of the thermal deformation in machine tools, Machine Tool & Hydraulics 5: 109-111.
2. **Ramesh, R.; Mannan, M.A.; Poo, A.N.** 2003. Thermal error measurement and modelling in machine tools. Part I. Influence of varying operating conditions, International Journal of Machine Tools & Manufacture 43: 391-404. http://dx.doi.org/10.1016/S0890-6955(02)00263-8.
3. **Tan Zhao, W.J.** 1997. Influence of thermal deformations of the machine on machining accuracy, Machine Tool 10: 1841-1844.
4. **Povilionis, A.; Bargelis, A**. 2010. Structural optimization in product design process, Mechanika 1(81): 66-70.
5. **Chen, J.S.** 1995. Computer-aided accuracy enhancement for multi-axis CNC machine tools, International Journal of Machine Tools and Manufacture 35(4): 593-605. http://dx.doi.org/10.1016/0890-6955(94)P4352-U.
6. **Cao, Y.J.** 2006. Research on errors recognition and compensation technology for the numerical control machine tools based on laser testing technology, Hangzhou: Zhejiang University.
7. **Zhang, Z.F.; Liu, Y.W;. Liu, L.B.** 2000. Thermal error modeling for five-axis NC machine based on multibody system theory, Journal of Hebei University of Technology 29(5): 23-28.
8. **Zhang, H.T.; Cao, H.T.; Shen, J.H.** 2006. Applica-

tion of artificial neural network theories in thermal error modeling and compensation of NC machine tools, Machinery 1: 17-20.
9. **Sun, H.Y.; Yang, J.G.** 2009. The research of thermal error compensation technology for turning center based on grey system theory, Modular Machine Tool & Automatic Manufacturing Technique, 7: 20-26.
10. **Wang, X.W.** 2010. Research on the thermal Error Compensation Technology for CNC Machine Tools. Taiyuan: North University of China.
11. **Ramesh, R.; Mannan, M.A.; Poo, A.N.** 2000. Error compensation in machine tools - a review Part II: thermal errors, International Journal of Machine Tools & Manufacture 40: 1257-1284. http://dx.doi.org/10.1016/S0890-6955(00)00010-9.
12. **Wu, H.; Zhang, H.T.; Guo, Q.J. et al.** 2008. Thermal error optimization modeling and real-time compensation on a CNC turning center, Journal of Materials Processing Technology 207: 172-179. http://dx.doi.org/10.1016/j.jmatprotec.2007.12.067.
13. **Lee, J.H.; Yang, S.H.** 2002. Statistical optimization and assessment of a thermal error model for CNC machine tools, International Journal of Machine Tools & Manufacture 42: 147-155. http://dx.doi.org/10.1016/S0890-6955(01)00110-9.
14. **Yu, Z.P.; Lu, Y.** 1995. Heat transfer theory. Beijing: Higher education press.
15. **Fan, M.W.** 2004. The finite element analysis of the thermal deformation on high-speed motorized spindle. Guangzhou: Guangdong University of technology.
16. **Hong, Q.L.; Yung, C.S.** 2004. Integrated dynamic thermo-mechanical modeling of high speed spindles, part 1: model development, Journal of Manufacturing Science and Engineering 126(1): 148-158. http://dx.doi.org/10.1115/1.1644545.
17. **Pei, D.M.** 2005. Research on the spindle system performance of the CNC double column boring and milling machine. Beijing: Tsinghua University.
18. **Chen, C.; Zhang, J.F.; Wu, Z.J.; Feng, P.F.** 2011. Real-time measurement of machine tool temperature fields and their effect on machining errors, Mechanika 17(4): 413-417. http://dx.doi.org/10.5755/j01.mech.17.4.572.

J. F. Zhang, P. F. Feng, Z. J. Wu, D. W. Yu, C. Chen

STAKLIŲ DARBINĖS GALVUTĖS ŠILUMINIŲ CHARAKTERISTIKŲ MODELIAVIMAS IR ANALIZĖ

R e z i u m ė

Šioje studijoje baigtinių elementų ir eksperimentiniais metodais ištirtos šilumos veikiamo tipinio apdirbimo centro eksploatacinės savybės, pasiūlytas metodas staklėms optimizuoti atsižvelgiant į struktūrines jų galvutės ir temperatūrinių laukų valdymo charakteristikas. Nekeičiant staklių šiluminių savybių ir statinio bei dinaminio standumo buvo pasinaudota simetrinės terminės plokštumos projektavimo teorija staklių galvutei optimizuoti į simetrinę struktūrą taip, kad šiluminės deformacijos būtų abipusiškai susietos ir panaudotos viena kitai kompensuoti. Aušinimo latakai buvo įtaisyti abiejose pusėse ir priekinėje galvutės dalyje, kad aušinimo valdymą būtų galima pritaikyti galvutės aušinimo latakų pločiui / gyliui ir išdėstymui optimizuoti. Todėl buvo galima pasiekti, kad staklės mažiau šiltų ir sumažėtų jų terminės deformacijos. Remiantis šilumos perdavimo suklio aušinimo latakams analizės duomenimis, buvo sukurtas terminio tinkamumo modeliavimo baigtiniais elementais metodas ir keliuose kritiniuose taškuose palyginta temperatūra ir visų staklių terminės deformacijos prieš optimizavimą ir po jo. Galiausiai, naudojant suprojektuotą ir pagal optimizavimo rezultatus pagamintą prototipą, buvo atlikti temperatūrinių eksploatacinių savybių eksperimentiniai matavimai. Lyginant modeliavimo ir eksperimento rezultatus buvo nustatyta, kad vertikaliojo apdirbimo centro temperatūrinės eksploatacinės savybės pagerėjo.

J. F. Zhang, P. F. Feng, Z. J. Wu, D. W. Yu, C. Chen

THERMAL STRUCTURE DESIGN AND ANALYSIS OF A MACHINE TOOL HEADSTOCK

S u m m a r y

In this study, it used a vertical machining center as the study object, conducted finite-element simulations and experimental research on its thermal performance, analyzed the weaknesses affecting the thermal performance of the machine tool, and proposed a machine tool thermal performance analysis method by combining structure optimization based on the headstock thermal characteristics and the temperature field control. Without changing the machine tool's heating power and static and dynamic stiffness, on the one hand, the design theory of the thermal plane of symmetry was used to reconstruct the headstock into a symmetrical structure such that the thermal deformations could be mutually coupled and offset each other. On the other hand, cooling troughs were designed on both sides and the front of the headstock so that cooling control could be arranged for the headstock by optimizing the layout and the width/depth of the cooling troughs. Therefore, the whole-machine temperature elevation and thermal deformation can be reduced. Based on the heat transfer analysis of the cooling troughs, it constructed a thermal performance finite-element simulation model and compared the temperature and whole-machine thermal deformation on several critical points before and after the reconstruction. Finally, the experimental measurements of the thermal performance were obtained using the prototype designed and manufactured based on the optimization results. It was verified that the thermal performance of the vertical machining center was greatly improved by comparing the simulation results with the experimental results.

Keywords: machine tool, headstock, temperature field, thermal deformation, reconstruction.

Received February 17, 2012
Accepted June 17, 2013